Insight into the GTPase Activity of Tubulin from Complexes with Stathmin-like Domains†

Chunguang Wang,‡,§,|| Anthony Cormier,‡,§ Benoît Gigant,§ and Marcel Knossow*,§

Laboratoire d'Enzymologie et Biochimie Structurales, CNRS, Bâtiment 34, Centre National de la Recherche Scientifique, 1 Avenue de la Terrasse, 91198 Gif-sur-Yvette Cedex, France, and Institute of Protein Research, Tongji University, 1239 Siping Road, Shanghai 200092, China

Received June 11, 2007; Revised Manuscript Received July 13, 2007

ABSTRACT: Microtubules are dynamically unstable tubulin polymers that interconvert stochastically between growing and shrinking states, a property central to their cellular functions. Following its incorporation in microtubules, tubulin hydrolyzes one GTP molecule. Microtubule dynamic instability depends on GTP hydrolysis so that this activity is crucial to the regulation of microtubule assembly. Tubulin also has a much lower GTPase activity in solution. We have used ternary complexes made of two tubulin molecules and one stathmin-like domain to investigate the mechanism of the tubulin GTPase activity in solution. We show that whereas stathmin-like domains and colchicine enhance this activity, it is inhibited by vinblastine and by the N-terminal part of stathmin-like domains. Taken together with the structures of the tubulin−colchicine−stathmin-like domain−vinblastine complex and of microtubules, our results lead to the conclusions that the tubulin−colchicine GTPase activity in solution is caused by tubulin−tubulin associations and that the residues involved in catalysis comprise the β tubulin GTP binding site and α tubulin residues that participate in intermolecular interactions in protofilaments. This site resembles the one that has been proposed to give rise to GTP hydrolysis in microtubules. The widely different hydrolysis rates in these two sites result at least in part from the curved and straight tubulin assemblies in solution and in microtubules, respectively.

Microtubules (MTs)[1] are cytoskeletal polymers of tubulin $\alpha\beta$ heterodimers involved in many cellular functions. Each tubulin subunit binds GTP. The GTP bound to the α subunit is nonhydrolyzable and nonexchangeable. The GTP bound to the β subunit is hydrolyzable and, in unassembled tubulin heterodimers, exchangeable. MTs assemble from tubulin with GTP in the β subunit (GTP-tubulin); this assembly is accompanied by GTP hydrolysis to GDP and P_i (*1*) but does not depend on it (*2*). By contrast, GTP hydrolysis controls the MT disassembly rate (*3*). A characteristic feature of MTs is the stochastic switching between growth and shrinking at their ends, a phenomenon termed dynamic instability (*4*). This allows quick reorganization of the microtubule cytoskeleton, such as from the interphase microtubule array to the mitotic spindle (*5*). Dynamic instability depends on GTP hydrolysis by tubulin as it is suppressed in MTs assembled in the presence of a slowly hydrolyzable analogue of GTP (*2*). Therefore, a complete understanding of the regulation of tubulin assembly requires a thorough investigation of the mechanism of tubulin GTPase activity, both structurally and mechanistically.

Structurally, the site for GTP hydrolysis in MTs has been well defined. It is mostly located in the tubulin β subunit and completed by α subunit residues upon the head-to-tail assembly of two heterodimers (*6*). Consistent with that, following GTP hydrolysis, GDP is sequestered in MTs at the tubulin exchangeable nucleotide site (*7*). By contrast, it has been difficult to characterize completely the kinetics of GTP hydrolysis during MT assembly. Indeed, steady-state rates have been measured by quantitating released phosphate upon MT assembly (*1, 8*), but as GTP hydrolysis occurs only close to MT ends, these measurements reflect the hydrolysis rate constant only if MT assembly is not rate-limiting. Such measurements have been achieved in the presence of Taxol (*8*) or of a microtubule-associated protein; in these conditions, when the number of GTP-hydrolyzing tubulin molecules could be estimated, rates larger than 7 s^{-1} have been determined (*9*).

Hydrolysis of GTP by soluble tubulin would seem to be a more appropriate system to characterize this catalytic activity if it were not for its very low rate. Binding of colchicine to tubulin significantly enhances this activity (*10*). Conditions have been found in which the corresponding specific activity depends on tubulin concentration (*11*); this has led to the proposal that GTP hydrolysis by tubulin in solution results from tubulin−tubulin collisions. This suggests that a defined tubulin assembly would be a good candidate for the characterization of this protein's GTPase

† Supported by ARC, La Ligue Contre le Cancer, and CNRS. C.W. was supported in part by an ARC postdoctoral fellowship.

* To whom correspondence should be addressed. Tel: 33 1 69 82 34 62. Fax: 33 1 69 82 31 29. E-mail: knossow@lebs.cnrs-gif.fr.

‡ These authors contributed equally to the work.

§ Laboratoire d'Enzymologie et Biochimie Structurales, CNRS.

|| Tongji University.

[1] Abbreviations: MT, microtubule; Rhel, fragment 46−138 of RB3-SLD; SLD, stathmin-like domain; Tc, tubulin−colchicine complex; $(Tc)_2R$, tubulin−colchicine−RB3-SLD complex; $(Tc)_2$Rhel, tubulin−colchicine−Rhel complex; T2R, tubulin−RB3-SLD complex; $(Tp)_2R$, tubulin−podophyllotoxin−RB3-SLD complex.

10.1021/bi701147f CCC: $37.00
Published on Web 08/21/2007

activity. The most extensively studied such assemblies result from the formation by tubulin of a complex with stathmin (*12*) or with the stathmin-like domains (SLDs) of proteins of the stathmin family. These are ternary complexes constituted of two tubulin heterodimers and one SLD (*13*), the only known possible exceptions being complexes of tubulin with *Drosophila* stathmin family proteins (*14*). These complexes are curved; their curvature results from a ca. 10° rotation that relates each tubulin subunit to the neighboring one (*15*, *16*). By contrast, in microtubule protofilaments, which are straight, tubulin subunits are related by a translation. Stathmin enhances the tubulin GTPase activity, in the presence of either colchicine (*17*) or significant amounts of glycerol (*18*).

Here we study the GTPase activity of the complex of tubulin−colchicine (Tc) with the SLD of the RB3 protein [$(Tc)_2R$]. We show that vinblastine, which inhibits the Tc GTPase activity (*10*), also inhibits that of $(Tc)_2R$. More surprisingly, the RB3-SLD N-terminal moiety (N-cap) also has a GTPase inhibitory effect. The crystal structure of $(Tc)_2R$ (*19*) shows that this RB3 peptide caps α tubulin residues that make longitudinal contacts in MTs and most likely in curved protofilaments. Therefore, our GTPase inhibition data imply that GTP hydrolysis by tubulin in solution results from the interaction of two heterodimers, one of them harboring the GTP binding site in its β subunit and the other one providing α subunit residues that enhance catalysis. These α tubulin residues comprise the conserved glutamate that has been proposed to accelerate GTP hydrolysis upon MT assembly (*6*). The observation that the hydrolysis rate in microtubules is much faster than at the assembled site in $(Tc)_2R$ shows that, for efficient GTP hydrolysis by tubulin, longitudinal tubulin assembly is not sufficient on its own and suggests that straight assembly is a prerequisite.

MATERIALS AND METHODS

Proteins and Buffers. Bovine brain tubulin was purified by two cycles of polymerization in a high molarity buffer (0.33 M PIPES-K, pH 6.9, 33% glycerol, 3.3 mM $MgCl_2$, 6.7 mM EGTA, 0.5 mM GTP, 1.5 mM ATP) (*20*) and depolymerization (in 50 mM Mes-K, pH 6.6, 1 mM $CaCl_2$, 1 mM 2-mercaptoethanol) and finally stored at −80 °C in 50 mM Mes-K, pH 6.8, 33% glycerol, 0.25 mM $MgCl_2$, 0.5 mM EGTA, and 0.1 mM GTP until use. Before each experiment, an additional MT assembly was performed, followed by disassembly in P buffer (80 mM PIPES-K, pH 6.8, 1 mM $MgCl_2$, 0.5 mM EGTA) containing 2 mM GDP; buffer was subsequently exchanged on a 8.3 mL bed volume Sephadex G-25 column (PD-10; Amersham) equilibrated in P buffer containing 20 μM GDP. The colchicine concentration was estimated from its absorbance at 351 nm (ϵ_{351} = 16218 mL cm^{-1} M^{-1}). Tubulin concentrations were deduced from its absorbance (ϵ_{278} = 1.23 mL cm^{-1} mg^{-1}), assuming the molecular mass of the heterodimer is 100 kDa (*21*). To prepare Tc, colchicine (Fluka) in excess (1 mM) was included in the depolymerization step in P buffer, and the unbound drug was removed on the following buffer exchange column. To check the efficiency of the buffer exchange, a solution of 2 mM GDP and 1 mM colchicine in P buffer was applied on the PD-10 column; the void volume of the column, where proteins elute, was effectively devoid of these small molecule compounds. The tubulin−colchicine stoichiometry was our main criteria to judge the quality of the Tc preparation; it was routinely 95% of the expected 1:1 ratio or better. RB3-SLD was expressed and purified as previously described (*13*), and the C-terminal helix of RB3 (Rhel, residues 46−138, stathmin numbering) was purified as described for similar fragments of stathmin (*22*). The SLD concentration was determined by amino acid analysis or by titrating a known tubulin solution with the SLD on a gel filtration column (Superose 12 10/300; Amersham). Both methods gave similar results. The $(tubulin-podophyllotoxin)_2$−RB3-SLD [$(Tp)_2R$] complex was prepared by incubating the $(tubulin)_2$−RB3-SLD complex with podophyllotoxin (Sigma) at a 100 μM concentration.

GTPase Activity Measurements. Tubulin at 10 μM was used for experiments in this study, except when otherwise stated. The GTPase activity of tubulin in the absence or presence of colchicine or podophyllotoxin and saturating amounts of RB3-SLD or Rhel (10 μM in most experiments) were measured at 37 °C in P buffer supplemented with 150 μM [γ-^{32}P]GTP (Amersham). For the measurements with vinblastine, the required amounts of vinblastine (Fluka) were incubated with $(Tc)_2R$ or $(Tc)_2$Rhel for at least 20 min at 4 °C. Measurements of the GTPase activity were started after prewarming the samples for 6 min at 37 °C. Free inorganic phosphate was quantified by extracting it as a phosphomolybdate complex as described (*23*). Briefly, 50 μL aliquots were taken off in the time course and mixed immediately with 1.5 mL of an ice-cold 10 mM ammonium molybdate solution in 1 M HCl and 4% $HClO_4$. H_3PO_4 (0.2 mM) was added as a carrier. After extraction by 3 mL of cyclohexane/isobutyl alcohol/acetone (5:5:1), 1 mL of the organic phase was mixed with 10 mL of scintillation solution for radioactivity counting. The radioactivity of 150 μM [γ-^{32}P]GTP was taken as a reference to calculate the quantity of GTP hydrolyzed. During the 24 min time course in which the reaction was monitored, the rate of GTP hydrolysis stayed constant. The slope of the plot of the concentration of inorganic phosphate as a function of time gives the total GTPase activity of each sample, and the average specific activity of tubulin was derived by dividing the background-subtracted total activity by the tubulin concentration.

In vinblastine inhibition experiments, since the $(Tc)_2R$−vinblastine complex does not hydrolyze GTP (see Results), the GTPase activity is proportional to the concentration of vinblastine-free $(Tc)_2R$. The binding of vinblastine to $(Tc)_2R$ was analyzed as shown in Scheme 1, where C is the $(Tc)_2R$−vinblastine complex.

Scheme 1

$$(Tc)_2R + V \rightleftharpoons C$$

Then

$$[C] = ([V]_0 + [T]_0 + K_D)/2 - ([([V]_0 + [T]_0 + K_D)/2]^2 - [V]_0[T]_0)^{1/2} \quad (1)$$

where $[V]_0$ and $[T]_0$ are the total concentrations of vinblastine and $(Tc)_2R$, respectively, and K_D is the dissociation constant of the $(Tc)_2R$−vinblastine complex. Within this scheme, upon vinblastine addition the GTPase activity is equal to k_{cat} ($[T]_0 - [C]$), where k_{cat} is the specific activity of $(Tc)_2R$.

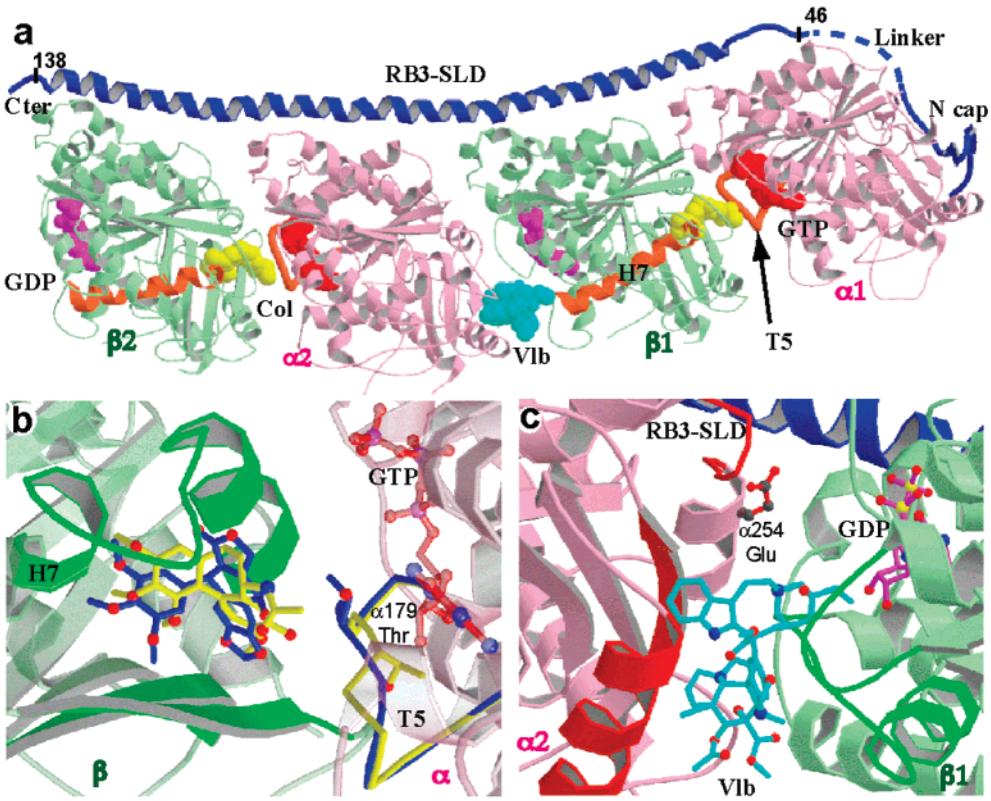

FIGURE 1: $(Tc)_2R$−vinblastine complex. (a) Overview. Ribbon representation of RB3-SLD and two tubulin $\alpha\beta$ heterodimers (PDB ID 1Z2B). The nucleotides (GTP on α, GDP on β), colchicine (Col, yellow), and vinblastine (Vlb, cyan) are shown as space-filling models. The dashed line shows the location of the RB3-SLD linker region, which is the least ordered part of RB3-SLD. Highlighted in orange are the α subunit T5 loops and the β subunit H7 helices (for a nomenclature of tubulin secondary structure elements, see ref *6*). RB3-SLD residues 46 and 138, which are the N- and C-terminal residues of Rhel, are labeled. (b) Close-up of the tubulin intradimer interface: nature of the colchicine-site ligand and conformation of the α T5 loop. The α1 (red) and β1 (green) subunits of $(Tc)_2R$ (PDB ID 1SA0) are presented as semitransparent ribbon diagrams; the colchicine binding site is in green. The T5 loop of the α subunit is highlighted (yellow) as well as the Thr α179 side chain, which change position depending on the bound ligand. Podophyllotoxin and the T5 loop (blue) of the α1 subunit of the $(Tp)_2R$ complex (PDB ID 1SA1) have been drawn after superimposition of the β1 subunits in this complex and in $(Tc)_2R$. Colchicine and podophyllotoxin are presented as ball-and-stick models in yellow and blue, respectively. (c) Close-up of the interdimer interface. The vinblastine binding site is highlighted in brighter colors in the α and β subunits. The α254 glutamate residue is represented as a ball-and-stick model. The distance from the carboxylate to the modeled γ-phosphate of the nucleotide is 7 Å. This figure was drawn with MOLSCRIPT (*40*) and RASTER3D (*41*).

Table 1: Tubulin GTPase Activity as a Function of the Bound Ligand and of Complexation with SLDs ($\times 10^{-3}$ min^{-1})

	ligand		
protein	none	colchicine	podophyllotoxin
tubulin	3.3 ± 0.2^a	7.5 ± 0.6^a	2.2 ± 0.2^a
T2R	3.4 ± 0.5^a	15.5 ± 0.7^a	3.2 ± 0.2^a
tubulin−Rhel complex	ND[b]	22.2 ± 0.5^a	ND[b]

[a] Errors were calculated from the deviations from a straight line of the variations of released P_i as a function of time in a single experiment, as described (*39*). They do not include other uncertainties such as batch to batch tubulin variations. The errors reported may therefore be underestimated. [b] Not determined.

Vinblastine Binding. The stoichiometry of vinblastine binding to $(Tc)_2R$ and the corresponding affinity were monitored by the quenching of $(Tc)_2R$ fluorescence using a Spex spectrofluorometer thermostated at 20 °C. Excitation and emission wavelengths were 280 mm and 340 nm, respectively. $(Tc)_2R$ (0.84 μM) in P buffer was reacted with varying amounts of vinblastine. Data were analyzed in terms of Scheme 1, which leads to a satisfactory fit of the observations ($R = 0.999$).

Structural Analysis. To compare the tubulin−podophyllotoxin and tubulin−colchicine structures, we superimposed the $(Tc)_2R$ and $(Tp)_2R$ crystal structures (PDB ID 1SA0 and 1SA1, respectively) using the program O (*24*). We performed additional refinement cycles in order to ascertain the conformation of regions potentially implicated in the GTPase mechanism and discussed in the text. To do so, we used the program Refmac (*25*) as in ref *19* except that the targeted residues were removed from the model prior to refinement. Resulting $F_o - F_c$ omit maps were visualized in O (see Supporting Information Figure 1 for an example).

RESULTS

Effect of RB3-SLD on Tubulin GTPase Activity. The GTPase activity was determined by incubating the complex formed by tubulin and RB3-SLD (T2R) with GTP, in the presence of either colchicine or podophyllotoxin. The site of these two drugs is located on the tubulin β subunit at the interface with α (see ref *19* and Figure 1). Colchicine stimulates the tubulin GTPase activity whereas podophyllotoxin leaves it essentially unchanged; in addition, whereas RB3-SLD slightly increases the average specific activity of the two podophyllotoxin-bound tubulin molecules in $(Tp)_2R$, it significantly enhances the Tc activity (Table 1). With these results in hand and since the binding of colchicine to tubulin

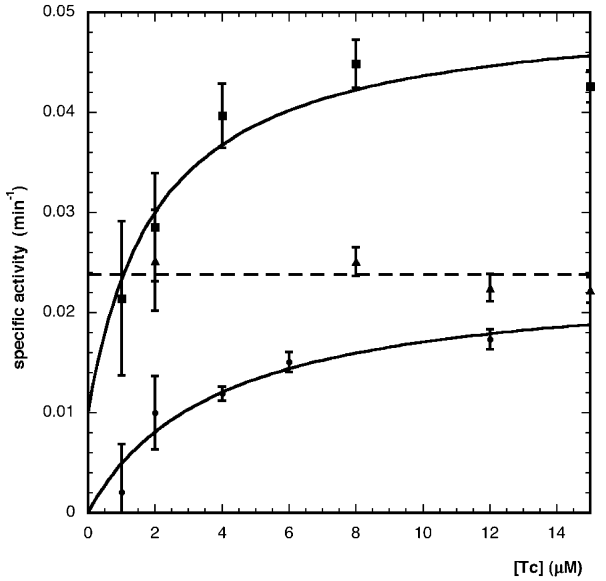

FIGURE 2: Variation of $(Tc)_2$Rhel specific activity as a function of its concentration. The GTPase activity of $(Tc)_2$Rhel (filled squares) was assayed in a high molarity (250 mM) PIPES buffer (see text), and the specific activity per Tc is presented as a function of Tc concentration. The variations of Tc and $(Tc)_2$R specific activities (filled circles and filled triangles, respectively) in the same buffer are also presented. Bars represent the uncertainty in the GTPase measurements. The curves are calculated according to the equation displayed in the Appendix, all residuals being smaller than 10% of the experimental values. The curve corresponding to the specific activity of $(Tc)_2$Rhel is obtained by adding a constant activity at the β1 site to the activity at the β2 end of the complex, which varies as a function of concentration. The quality of the fit only slightly depends on the value of the β1 site activity; therefore, the curve presented is only one of the possible choices yielding similar fits. The dashed line is the best fit of $(Tc)_2$R activity by a constant.

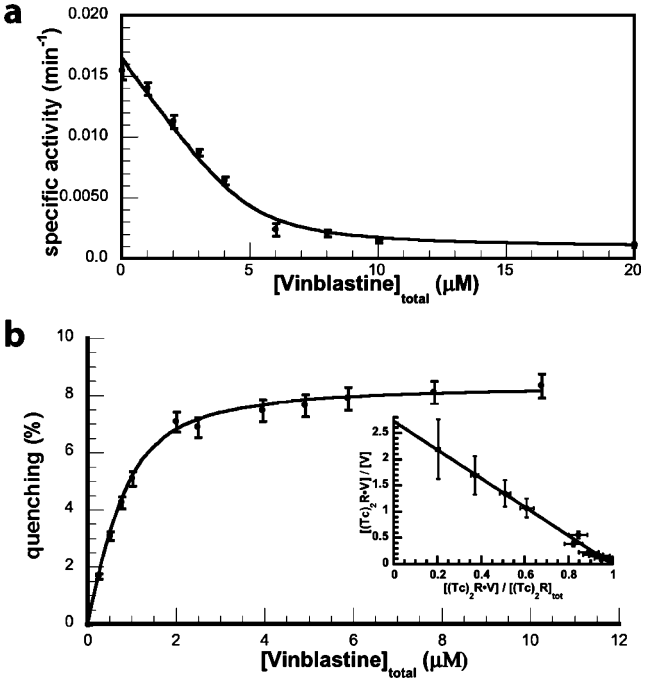

FIGURE 3: Biochemical consequences of $(Tc)_2$R−vinblastine interactions. (a) Inhibition of the $(Tc)_2$R GTPase activity by vinblastine. Experimental values of the average tubulin activity (tubulin concentration: 10 μM) are accounted for by the binding of vinblastine to $(Tc)_2$R as described in Materials and Methods (eq 1). The variations of the GTPase activity are represented as a function of the total (bound and unbound) vinblastine concentration. The best fit to the data (continuous line) is based on eq 1. (b) Quenching of $(Tc)_2$R fluorescence by vinblastine. The variations of fluorescence quenching are presented as a function of the total (bound and unbound) vinblastine concentration. Insert: Corresponding Scatchard plot.

is well characterized (*19*, *26*, *27*), we chose to study the Tc GTPase activity.

We next examined the GTPase activity of the complex of Tc with Rhel and found that it is significantly higher than in the complex with RB3-SLD (Table 1). Rhel consists mainly of the RB3-SLD C-terminal α-helix contacting tubulin all along T2R; it lacks the N-cap, a two-stranded β-sheet at the N-terminal end of RB3-SLD, and most of the linker from this region to the C-terminal α-helix (Figure 1a). Since Rhel lacks some of the RB3-SLD elements that contact tubulin, its affinity for tubulin is expected to be lower than that of RB3-SLD. We therefore checked that virtually all of the tubulin was complexed to Rhel. Since the activity of Tc is smaller than that measured in the presence of Rhel (by a factor of 3; see Table 1), it suffices to check whether the overall GTPase activity is augmented when the concentration of Rhel is increased. We verified that when the concentration of Rhel is tripled, the $(Tc)_2$Rhel GTPase activity is unchanged (data not shown); this demonstrates that all Tc is bound to Rhel under the conditions used (10 μM tubulin concentration and a 2-fold excess of Rhel, i.e., a 10 μM concentration). We also measured the variations of $(Tc)_2$R and $(Tc)_2$Rhel specific GTPase activities as a function of tubulin concentration. We find that, in the 2−15 μM tubulin concentration range, the $(Tc)_2$R and $(Tc)_2$Rhel specific activities are respectively within a factor of 1.0 ± 0.09 and 0.98 ± 0.07 of their value at a 10 μM tubulin concentration. By contrast, when assayed in a buffer with a higher PIPES content than the P buffer (250 vs 80 mM), the specific activity of $(Tc)_2$Rhel, as well as that of Tc, is enhanced and depends on tubulin concentration whereas the specific activity of $(Tc)_2$R does not (Figure 2).

There are two hydrolyzable GTP sites in $(Tc)_2$R, both in tubulin β subunits. One is at the interface of the two heterodimers; the other one is at the end of the $(Tc)_2$R complex opposite to the RB3-SLD N-cap (Figure 1a). The additional activity of $(Tc)_2$Rhel compared to $(Tc)_2$R could be due to an increase of hydrolysis at one of the hydrolyzable GTP sites or to a change at both. The study of the inhibition of the $(Tc)_2$R and $(Tc)_2$Rhel GTPase activities by vinblastine and further characterization of the corresponding complexes with vinblastine allowed us to distinguish between these two possibilities.

Inhibition of the $(Tc)_2$R and $(Tc)_2$Rhel GTPase Activities by Vinblastine. Vinblastine inhibits the Tc GTPase activity (*10*) and induces its isodesmic helical polymerization (*28*). We have previously characterized the binding of vinblastine to $(Tc)_2$R both structurally and kinetically (*29*). Here we find that vinblastine quantitatively inhibits the $(Tc)_2$R GTPase activity. The variation of this activity as a function of vinblastine concentration is perfectly accounted for by the binding of one vinblastine molecule to $(Tc)_2$R according to Scheme 1 (Figure 3a). The 0.34 ± 0.19 μM dissociation constant deduced from the inhibition curve (Figure 3a) is identical, within experimental error, to the one we have calculated from the ratio of the $(Tc)_2$R−vinblastine dissociation and association rate constants (0.4 ± 0.3 μM) (*29*). In

addition, we probed vinblastine binding by examining the resulting $(Tc)_2R$ fluorescence quenching (Figure 3b) and found that this also is perfectly accounted for by Scheme 1, with a dissociation constant (0.31 ± 0.03 μM) identical to the one we have deduced from the inhibition of the $(Tc)_2R$ GTPase activity. The linear Scatchard plot of these data (Figure 3b) is consistent with the fluorescence change being linked to vinblastine binding to a single site in the concentration range we have explored. We have shown (*29*) that one vinblastine site in $(Tc)_2R$ is equally contributed to by the α and β subunits of the two tubulin molecules of the complex (Figure 1c); it is located close to the β1 tubulin hydrolyzable GTP, the distance between the closest atoms of vinblastine and β1 GDP being 7 Å. There is a second potentially hydrolyzable GTP in $(Tc)_2R$, at the β2 end; it is close to a partial vinblastine site which lacks the contribution of α subunit residues so that binding to that site is expected to be much weaker than binding at the β1−α2 interface. The inhibition of the $(Tc)_2R$ GTPase activity and fluorescence quenching by vinblastine data demonstrate that this drug binds to a high-affinity site. We conclude from the comparison of the two potential vinblastine sites that this is the site at the interface of the two heterodimers (Figure 1a), as defined in the structure of the $(Tc)_2R$−vinblastine complex (*29*).

This observation allows us to define more accurately the enhancement of Tc GTPase rate by RB3-SLD. The rate of tubulin GTPase activity in $(Tc)_2R$ is enhanced by a factor of 2 as compared to Tc (Table 1). This represents an average over the two hydrolyzable nucleotide sites in the complex, but these are not equivalent: one is contacted by an α tubulin subunit whereas the second one contacts the solvent. As all GTP hydrolysis is inhibited by vinblastine binding at the β1−α2 interface, we conclude that GTP hydrolysis by $(Tc)_2R$ occurs solely at that site and that the β2 tubulin nucleotide is not hydrolyzed in these conditions. The same finding, using a different experimental approach, has been reported previously (*18*). The enhancement factor in $(Tc)_2R$ for GTP hydrolysis at the β1 tubulin subunit site is 4, the corresponding rate being 3.2×10^{-2} min^{-1}.

We also measured the inhibition of $(Tc)_2Rhel$ GTPase activity by vinblastine, in parallel to that of $(Tc)_2R$, using the same batch of tubulin. The inhibition of $(Tc)_2Rhel$ GTPase activity is virtually complete, but it requires a higher concentration of vinblastine to achieve than in $(Tc)_2R$ (Figure 4). Interestingly, the difference between $(Tc)_2R$ and $(Tc)_2Rhel$ GTPase activities stays constant as a function of vinblastine concentration up to the nearly complete inhibition of an activity equal to that of $(Tc)_2R$ (Figure 4). The simplest interpretation is that there are two different binding sites for vinblastine in $(Tc)_2Rhel$ with significantly different affinities. At low concentration vinblastine binds to a high-affinity site and inhibits an activity equal to that of $(Tc)_2R$, which suggests that this is the vinblastine site identified in $(Tc)_2R$ at the interface of the two tubulin heterodimers (*29*). At high vinblastine concentration, the difference between vinblastine-inhibited $(Tc)_2Rhel$ and $(Tc)_2R$ activities decreases. As this difference is not affected by vinblastine until the activity arising from the first site is inhibited, we propose that it is due to GTPase activity at a site for which vinblastine's affinity is low. Comparison of the two vinblastine sites in $(Tc)_2R$ leads us to conclude that this is likely to be the β2 subunit site. This is also consistent with the observation that this drug induces the formation of $(Tc)_2Rhel$ helical aggregates whose shape is accounted for by the vinblastine-mediated head to tail assembly of $(Tc)_2Rhel$ complexes, most likely through the binding at the interface of the β2 subunit of one complex and of the α1 subunit of the neighboring one (*29*). Inhibition of the extra GTPase activity of $(Tc)_2Rhel$ compared to $(Tc)_2R$ at high vinblastine concentration suggests that, as opposed to $(Tc)_2R$, the β2 GTP is hydrolyzed in $(Tc)_2Rhel$.

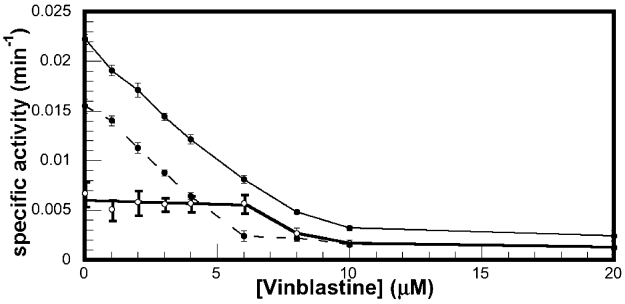

FIGURE 4: Inhibition of the $(Tc)_2Rhel$ GTPase activity by vinblastine. The average tubulin activity in $(Tc)_2Rhel$ (closed circles connected by a thin solid line), as well as in $(Tc)_2R$ (closed circles connected by a dashed line) and the difference between them (open circles) are represented as a function of vinblastine concentration. At vinblastine concentrations smaller than 6 μM, the difference between $(Tc)_2Rhel$ and $(Tc)_2R$ GTPase activities stays constant, with the linear fit (thick solid line) nearly parallel to the abscissa axis. At vinblastine concentrations higher than 6 μM, the line joins the activity difference data points.

Because of the different results obtained with $(Tc)_2R$ and $(Tc)_2Rhel$, we measured the $(Tc)_2Rhel$ GTPase activity in the presence of a stathmin peptide homologous to the RB3-SLD N-cap (*19*). Taken together, the RB3-SLD N-cap (residues 4−25) and Rhel (residues 46−138) constitute most of RB3-SLD, the main missing part being the linker between these two peptides. The stathmin peptide (residues 5−24) has been shown by NMR to bind to tubulin and to adopt then the same β-hairpin structure as its RB3 homologue in $(Tc)_2R$ (*30*). We chose the stathmin peptide rather than its RB3 counterpart as it has a higher affinity for tubulin (*30*). We find that 1 mM peptide inhibits $(Tc)_2Rhel$ GTPase activity to the level of that of $(Tc)_2R$, the ratio between these activities being 1.1 ± 0.15.

Comparison of the Tubulin−Colchicine and Tubulin−Podophyllotoxin Structures. The $(Tc)_2R$ and $(Tp)_2R$ structures are highly isomorphous: the root mean square deviation of Cα positions is 0.55 Å after αβ tubulin superposition, to be compared to 0.53 and 0.4 Å when the α and β subunits are superimposed separately. This means that the structures of tubulin subunits are highly isomorphous but also that their relative orientations are the same in the two complexes. The only significant difference between the two structures, apart from the different ligands, is a different conformation of the T5 loop of the α tubulin subunit (Figure 1b and Supporting Information Figure 1). This loop, which is located close to the colchicine−podophyllotoxin site, is highly variable as its conformation in Zn-sheet tubulin protofilaments (*31*) differs from the two conformations it adopts in $(Tc)_2R$ and $(Tp)_2R$. In T2R, there are two such loops and two ligand sites, harboring colchicine or podophyllotoxin. The T2R β subunit nucleotides, the only nucleotides that may be hydrolyzed, are located at least 20 Å away from the T5 loops

and colchicine−podophyllotoxin site. There may nevertheless be a structural link between colchicine (or podophyllotoxin) and the hydrolyzable nucleotide as they both contact the H7 central helix, at its C-terminal end and its N-terminal end, respectively (Figure 1a,b).

DISCUSSION

In this study we have characterized the tubulin GTPase activity in solution and its modulation by tubulin ligands, in a defined structural context. This allows us to describe the corresponding active site and to compare it with the site for GTP hydrolysis that follows MT assembly.

Mechanism of Tubulin GTPase Activity. Our results strongly suggest that in $(Tc)_2$Rhel the β2 subunit GTP is hydrolyzed, by contrast to what is observed in $(Tc)_2$R. This leads us to propose that transient protofilament-like $(Tc)_2$Rhel assemblies give rise to the additional GTPase activity of $(Tc)_2$Rhel as compared to $(Tc)_2$R. Indeed, the only difference between the two complexes is that in $(Tc)_2$Rhel the N-cap of RB3-SLD is missing. The RB3-SLD N-cap contacts α tubulin subunit residues that participate in intermolecular (longitudinal) contacts in protofilaments when tubulin assembles in MTs (*32*). They are masked in $(Tc)_2$R and become exposed in $(Tc)_2$Rhel. The RB3-SLD N-cap is located more than 160 Å away from the β2 subunit nucleotide (*19*), so that it is unlikely to influence this nucleotide's reactivity through a pathway that would have to cross the whole $(Tc)_2$Rhel complex. By contrast, the tubulin residues unmasked in $(Tc)_2$Rhel would come close to the β2 subunit GTP site of another complex as they assemble head to tail, transiently, in a protofilament-like manner. Consistent with this, the stathmin N-terminal peptide inhibits the $(Tc)_2$Rhel GTPase activity, bringing it down to the level of the GTPase activity of $(Tc)_2$R.

Similarly, collisions have been suggested to give rise to Tc GTPase activity (*11*). We propose that, in solution, the α subunit residues of one tubulin molecule that are masked in $(Tc)_2$R by the RB3 N-cap enhance tubulin's GTPase activity in another heterodimer. These α tubulin residues comprise the invariant Glu 254 which, based on structural data (*6*), on mutational analysis in yeast (*33*), and on mutational analysis of the bacterial tubulin homologue FtsZ (*34*), has been proposed to assist GTP hydrolysis in MTs. As tubulin's GTPase activity results from the overall structure of an active site constituted of a β subunit nucleotide site and of an α subunit moiety that belongs to another heterodimer, it is not surprising that this activity depends significantly on the context in which it is measured. It is low in Tc and enhanced by a factor of 4 in $(Tc)_2$R where both moieties are held together in space. In MTs, rate estimates at least 10000 times faster than in solution have been provided in conditions where assembly is faster than GTP hydrolysis and when the number of GTP hydrolyzing molecules could be defined (*8*, *9*). The much faster rate in MTs raises the question of the similarities of the mechanisms for GTP hydrolysis in MTs and in solution. As the sites involved comprise similar residues, one contributing factor to the rate difference is likely to be the different geometries of these sites. The α subunit Glu 254 is closer to the nucleotide phosphates in straight protofilaments than in curved assemblies, the distance to a modeled γ phosphate being 4 Å compared to ca. 7 Å in $(Tc)_2$R. Better positioning of α subunit residues, including Glu 254, would contribute to the considerably increased reaction rate of the β subunit nucleotide in straight protofilaments.

The proposal that the additional specific GTPase activity of $(Tc)_2$Rhel compared to $(Tc)_2$R arises from intermolecular interactions leads to the possibility that this activity would depend on $(Tc)_2$Rhel concentration, which we observe only in a high concentration PIPES buffer. In a model for Tc GTPase activity in solution that has been proposed (*11*), interactions of unactivated molecules lead to activation of the GTPase activity whereas interactions of Tc with an activated species lead to deactivation of the GTPase activity. According to this model, the dependence of the Tc specific activity on its concentration is significant only if the hydrolysis rate constant of the activated species (k_h) cannot be neglected compared to the frequency of deactivating interactions; this frequency is proportional to Tc concentration. In the case of $(Tc)_2$Rhel and in P buffer, k_h is too low for a dependence of its specific activity on concentration to be observed in the range where meaningful measurements are practical (see Appendix). But in conditions where the $(Tc)_2$Rhel specific activity, as well as that of Tc, is significantly enhanced, we do observe such a dependence (see Figure 2). In these conditions, at high PIPES molarity, significant amounts of assembled $(Tc)_2$Rhel (or Tc) that have GTPase activity are detected by centrifugation (data not shown). It is therefore conceivable that in a high molarity PIPES buffer tubulin assemblies similar to those previously described (ref *35* and references therein) are more abundant than in the usual conditions where GTPase activity is assayed, which leads to the observed enhanced, tubulin concentration dependent, activity. Leveling off of the specific activity at high tubulin concentration might be due to further interactions with tubulin which would lead to less flexible complexes with lower activity, similar to the effect of vinblastine binding (see below).

We, as others, find that whereas Tc has a significant GTPase activity, those of tubulin and tubulin−podophyllotoxin are much lower (*10*). We also find that the effect of RB3-SLD on tubulin and tubulin−podophyllotoxin is significantly less pronounced than on Tc (Table 1). The observation that, apart from the ligands, the main difference between the two structures lies in the different conformations of the α subunit T5 loops (see above and ref *19*) leads to the intriguing possibility that the hydrolysis observed is that of the α subunit GTP. We discard the possibility that what we measure is the colchicine-induced hydrolysis of the nearby α tubulin GTP for three main reasons: (i) there is no evidence for it in the $(Tc)_2$R crystals though crystals have been standing at room temperature for days before diffraction data collection; (ii) such a hydrolysis would be hard to reconcile with the observed inhibition by vinblastine, which binds 44 Å away from the α tubulin GTP when no transmitting structural change is detected between vinblastine and this nucleotide; (iii) to measure any radioactive P_i produced at the α tubulin GTP site, exchange of GTP by radiolabeled GTP needs to occur during the 30 min period when tubulin is exposed to it whereas exchange of the α tubulin nucleotide in a 1 h period has been shown to be negligible (*36*). Moreover, the linearity of the release of P_i as a function of time suggests that GTP exchange is not rate

limiting in our conditions. The α subunit T5 loop, which has the same conformation in tubulin−podophyllotoxin and unliganded tubulin (data not shown) and a different one in Tc, may have a long-range effect on residues in the same α subunit that assist catalysis. This conformational switch is one possible candidate for the structural rearrangement that has been postulated to be required for a significant GTPase activity of nonmicrotubular tubulin (see ref *37* and references therein). Alternatively, it is conceivable that the different GTPase activities of Tc and tubulin−podophyllotoxin arise from subtle differences among the contacts of colchicine and podophyllotoxin with the H7 β tubulin helix whose effects would be passed along the helix to the β subunit nucleotide binding site. Other possibilities cannot be ruled out. One of them would be that the difference between the GTP−tubulin colchicine and podophyllotoxin complexes is more significant than that between the complexes of GDP−tubulin with these compounds, which are the only complexes for which structural data are available.

Mechanism for the Inhibition of Tubulin−Colchicine GTPase Activity by Vinblastine. Vinblastine binds to $(Tc)_2R$ at the $\beta1-\alpha2$ interface (Figure 1c). In $(Tc)_2R$ this interface is flexible, as the angle of the rotation that superimposes the $\beta1$ and $\alpha2$ subunits varies between 7° and 14° in the $(Tc)_2R$ crystals we have studied (unpublished observations). This flexibility would allow proper positioning of $\alpha2$ subunit residues to enhance $\beta1$ subunit GTPase activity. Vinblastine as it acts as a wedge at the $\beta1-\alpha2$ interface restricts this flexibility, which likely explains its inhibitory effect. There are also some local changes at the tubulin−tubulin interface in $(Tc)_2R$ following vinblastine binding (*29*) which may affect GTP hydrolysis. It is tempting to suggest that vinblastine inhibits Tc GTPase activity (*10*) by a mechanism similar to the one we just described. We propose that, when bound to tubulin, vinblastine prevents proper positioning of α subunit residues in one tubulin heterodimer relative to the GTP in another molecule to enhance its GTPase activity.

Biological Implications. As a consequence of GTP hydrolysis by tubulin following MT assembly, the dependence of the assembly rate on tubulin concentration is strikingly nonlinear close to the tubulin critical concentration (*3*). This results in MT dynamic instability (*4*), an important consequence of GTP hydrolysis by tubulin. Stathmin-like proteins, which regulate MT assembly, sequester two tubulin molecules as a head-to-tail assembly in which the average GTP hydrolysis over the two tubulins is essentially unchanged unless colchicine is bound to tubulin (Table 1). In any case, the rate is probably at least 10000 times slower than that of GTP hydrolysis in MTs (*8*, *9*). In $(Tc)_2R$, in Tc, and in MTs, GTP hydrolysis by one tubulin heterodimer is enhanced by residues of another one, suggesting that, despite the different specific activities, the mechanisms share common features. But, for rapid hydrolysis of a β tubulin GTP, the assistance of another heterodimer's α subunit residues, positioned as in straight protofilaments, is required. This ensures that the effect of futile cycles of GTP hydrolysis by tubulin is minimized, even when it is complexed to a MT regulatory protein such as a stathmin family protein.

In addition to these results, our work has a more practical possible application concerning tubulin's Vinca domain ligands, which are extensively studied because of their antimitotic properties (*38*). We have shown here that $(Tc)_2R$ GTPase inhibition is a convenient way to measure the interaction of tubulin with these ligands, which would complement X-ray structural studies of their complexes with $(Tc)_2R$. Both types of experiments are made practical because, as opposed to tubulin, $(Tc)_2R$ is not prone to aggregation by Vinca site ligands (*29*).

ACKNOWLEDGMENT

We gratefully acknowledge M.-F. Carlier for help and discussions, A. Sobel for generous gifts of materials, and F. Jacquinot and A. Vigouroux for excellent assistance.

APPENDIX

A model in which interactions between $(Tc)_2$Rhel complexes lead to activation to a state that either hydrolyzes the $\beta2$ subunit GTP with a first-order rate constant k_h or, alternatively, deactivates through another interaction with $(Tc)_2$Rhel leads to the following steady-state rate of $\beta2$ subunit GTP hydrolysis, similar to what has been proposed for Tc (*11*):

$$v = k_h k_+ \frac{[(Tc)_2Rhel]^2}{k_-[(Tc)_2Rhel] + k_h}$$

where k_+ and k_- are the activation and deactivation rate constants.

According to this equation, when $[(Tc)_2Rhel]$ is large so that the specific rate $v/[(Tc)_2Rhel]$ does not depend on it, this rate is equal to $k_h(k_+/k_-)$. Assuming that the $(Tc)_2$Rhel activation rate constant, k_+, is similar to that calculated for Tc (0.015 μM^{-1} min^{-1}) (*11*) and that the specific rate constant at the $\beta2$ site is equal to the difference of the specific rate constants of $(Tc)_2$Rhel and $(Tc)_2R$, i.e., $6.7 \pm 1.2 \times 10^{-3}$ min^{-1} (Table 1, where measurements are made at 10 μM tubulin concentration), we deduce that k_h/k_- is equal to 0.4 μM. This means that at the lowest $(Tc)_2$Rhel concentration where rates were measured (2 μM tubulin, i.e., 1 μM $(Tc)_2$Rhel), the ratio $k_h/(k_-[(Tc)_2Rhel])$ is equal to 0.4, a value similar to the calculated relative error (0.39) on the measurement of the specific rate at the $\beta2$ site when this measurement is made at 2 μM tubulin concentration. Consequently, in the range of $(Tc)_2$Rhel concentrations where measurements in P buffer are practical, the variation of this specific rate is similar to experimental uncertainties.

SUPPORTING INFORMATION AVAILABLE

One figure describing the conformations of the α tubulin T5 loop in $(Tc)_2R$ and $(Tp)_2R$. This material is available free of charge via the Internet at http://pubs.acs.org.

REFERENCES

1. Vandecandelaere, A., Brune, M., Webb, M. R., Martin, S. R., and Bayley, P. M. (1999) Phosphate release during microtubule assembly: what stabilizes growing microtubules?, *Biochemistry 38*, 8179−8188.
2. Hyman, A. A., Salser, S., Drechsel, D. N., Unwin, N., and Mitchison, T. J. (1992) Role of GTP hydrolysis in microtubule dynamics: information from a slowly hydrolyzable analogue, GMPCPP, *Mol. Biol. Cell 3*, 1155−1167.
3. Carlier, M. F., Hill, T. L., and Chen, Y. (1984) Interference of GTP hydrolysis in the mechanism of microtubule assembly: an experimental study, *Proc. Natl. Acad. Sci. U.S.A. 81*, 771−775.

4. Mitchison, T. J., and Kirschner, M. W. (1984) Dynamic instability of microtubule growth, *Nature 312*, 237−242.
5. Desai, A., and Mitchison, T. J. (1997) Microtubule polymerization dynamics, *Annu. Rev. Cell Dev. Biol. 13*, 83−117.
6. Nogales, E., Downing, K. H., Amos, L. A., and Löwe, J. (1998) Tubulin and FtsZ form a distinct family of GTPases, *Nat. Struct. Biol. 5*, 451−458.
7. David-Pfeuty, T., Erickson, H. P., and Pantaloni, D. (1977) Guanosinetriphosphatase activity of tubulin associated with microtubule assembly, *Proc. Natl. Acad. Sci. U.S.A. 74*, 5372−5376.
8. Melki, R., Fievez, S., and Carlier, M. F. (1996) Continuous monitoring of Pi release following nucleotide hydrolysis in actin or tubulin assembly using 2-amino-6-mercapto-7-methylpurine ribonucleoside and purine-nucleoside phosphorylase as an enzyme-linked assay, *Biochemistry 35*, 12038−12045.
9. Burns, R. G. (1991) Kinetics of GTP hydrolysis during the assembly of chick brain MAP2-tubulin microtubule protein, *Biochem. J. 277* (Part 1), 239−243.
10. David-Pfeuty, T., Simon, C., and Pantaloni, D. (1979) Effect of antimitotic drugs on tubulin GTPase activity and self-assembly, *J. Biol. Chem. 254*, 11696−11702.
11. Heusele, C., and Carlier, M. F. (1981) GTPase activity of the tubulin-colchicine in relation with tubulin-tubulin interactions, *Biochem. Biophys. Res. Commun. 103*, 332−338.
12. Jourdain, L., Curmi, P., Sobel, A., Pantaloni, D., and Carlier, M.-F. (1997) Stathmin is a tubulin sequestering protein which forms a ternary T2S complex with two tubulin molecules, *Biochemistry 36*, 10817−10821.
13. Charbaut, E., Curmi, P. A., Ozon, S., Lachkar, S., Redeker, V., and Sobel, A. (2001) Stathmin family proteins display specific molecular and tubulin binding properties, *J. Biol. Chem. 276*, 16146−16154.
14. Ozon, S., Guichet, A., Gavet, O., Roth, S., and Sobel, A. (2002) *Drosophila* stathmin: a microtubule-destabilizing factor involved in nervous system formation, *Mol. Biol. Cell 13*, 698−710.
15. Gigant, B., Curmi, P. A., Martin-Barbey, C., Charbaut, E., Lachkar, S., Lebeau, L., Siavoshian, S., Sobel, A., and Knossow, M. (2000) The 4 Å X-ray structure of a tubulin:stathmin-like domain complex, *Cell 102*, 809−816.
16. Steinmetz, M. O., Kammerer, R. A., Jahnke, W., Goldie, K. N., Lustig, A., and van Oostrum, J. (2000) Op18/stathmin caps a kinked protofilament-like tubulin tetramer, *EMBO J. 19*, 572−580.
17. Amayed, P., Carlier, M. F., and Pantaloni, D. (2000) Stathmin slows down guanosine diphosphate dissociation from tubulin in a phosphorylation-controlled fashion, *Biochemistry 39*, 12295−12302.
18. Brannstrom, K., Segerman, B., and Gullberg, M. (2003) Molecular dissection of GTP exchange and hydrolysis within the ternary complex of tubulin heterodimers and Op18/stathmin family members, *J. Biol. Chem. 278*, 16651−16657.
19. Ravelli, R. B., Gigant, B., Curmi, P. A., Jourdain, I., Lachkar, S., Sobel, A., and Knossow, M. (2004) Insight into tubulin regulation from a complex with colchicine and a stathmin-like domain, *Nature 428*, 198−202.
20. Castoldi, M., and Popov, A. V. (2003) Purification of brain tubulin through two cycles of polymerization-depolymerization in a high-molarity buffer, *Protein Expression Purif. 32*, 83−88.
21. Correia, J. J., Baty, L. T., and Williams, R. C., Jr. (1987) Mg^{2+} dependence of guanine nucleotide binding to tubulin, *J. Biol. Chem. 262*, 17278−17284.
22. Redeker, V., Lachkar, S., Siavoshian, S., Charbaut, E., Rossier, J., Sobel, A., and Curmi, P. A. (2000) Probing the native structure of stathmin and its interaction domains with tubulin, *J. Biol. Chem. 275*, 6841−6849.
23. Carlier, M. F., Didry, D., and Pantaloni, D. (1987) Microtubule elongation and guanosine 5′-triphosphate hydrolysis. Role of guanine nucleotides in microtubule dynamics, *Biochemistry 26*, 4428−4437.
24. Jones, T. A., Zhou, J.-Y., Cowan, S. W., and Kjeldgaard, M. (1991) Improved methods for building protein models in electron density maps and the location of errors in these models, *Acta Crystallogr. A 47*, 110−119.
25. Winn, M. D., Isupov, M. N., and Murshudov, G. N. (2001) Use of TLS parameters to model anisotropic displacements in macromolecular refinement, *Acta Crystallogr. D 57*, 122−133.
26. Engelborghs, Y. (1998) General features of the recognition by tubulin of colchicine and related compounds, *Eur. Biophys. J. 27*, 437−445.
27. Garland, D. L. (1978) Kinetics and mechanism of colchicine binding to tubulin: evidence for ligand-induced conformational change, *Biochemistry 17*, 4266−4272.
28. Weisenberg, R. C., and Timasheff, S. N. (1970) Aggregation of microtubule subunit protein. Effects of divalent cations, colchicine and vinblastine, *Biochemistry 9*, 4110−4116.
29. Gigant, B., Wang, C., Ravelli, R. B., Roussi, F., Steinmetz, M. O., Curmi, P. A., Sobel, A., and Knossow, M. (2005) Structural basis for the regulation of tubulin by vinblastine, *Nature 435*, 519−522.
30. Clément, M.-J., Jourdain, I., Lachkar, S., Savarin, P., Gigant, B., Knossow, M., Toma, F., Sobel, A., and Curmi, P. A. (2005) N-terminal Stathmin-like peptides bind tubulin and impede microtubule assembly, *Biochemistry 44*, 14616−14625.
31. Löwe, J., Li, H., Downing, K. H., and Nogales, E. (2001) Refined structure of alpha beta tubulin at 3.5 Å resolution, *J. Mol. Biol. 313*, 1045−1057.
32. Nogales, E., Whittaker, M., Milligan, R. A., and Downing, K. H. (1999) High-resolution model of the microtubule, *Cell 96*, 79−88.
33. Anders, K. R., and Botstein, D. (2001) Dominant-lethal alpha-tubulin mutants defective in microtubule depolymerization in yeast, *Mol. Biol. Cell 12*, 3973−3986.
34. Dai, K., Mukherjee, A., Xu, Y., and Lutkenhaus, J. (1994) Mutations in ftsZ that confer resistance to SulA affect the interaction of FtsZ with GTP, *J. Bacteriol. 176*, 130−136.
35. Saltarelli, D., and Pantaloni, D. (1982) Polymerization of the tubulin-colchicine complex and guanosine 5′-triphosphate hydrolysis, *Biochemistry 21*, 2996−3006.
36. Weisenberg, R. C., Borisy, G. G., and Taylor, E. W. (1968) The colchicine-binding protein of mammalian brain and its relation to microtubules, *Biochemistry 7*, 4466−4479.
37. Perez-Ramirez, B., Shearwin, K. E., and Timasheff, S. N. (1994) The colchicine-induced GTPase activity of tubulin: state of the product. Activation by microtubule-promoting cosolvents, *Biochemistry 33*, 6253−6261.
38. Jordan, M. A., and Wilson, L. (2004) Microtubules as a target for anticancer drugs, *Nat. Rev. Cancer 4*, 253−265.
39. Bevington, P. R., and Robinson, K. D. (1992) *Data reduction and error analysis for the physical sciences*, 2nd ed., McGraw-Hill, New York.
40. Kraulis, P. (1991) MOLSCRIPT: a program to produce both detailed and schematic plots of proteins structures, *J. Appl. Crystallogr. 24*, 946−950.
41. Merritt, E. A., and Murphy, M. E. P. (1994) Raster3D version 2.0. A program for photorealistic molecular graphics, *Acta Crystallogr. D 50*, 869−873.

BI701147F